New Tridentate Ligand Affords Long-Lived ^{3}MLCT Excited State in a Ru(II) Complex: DNA Photocleavage and $^1O_2$ Production

Austin P. Lanquist,[‡] Eric J. Piechota,[‡] Lanka D. Wickramasinghe,[†] Alexia Marques Silva,[‡] Randolph P. Thummel,[†]* and Claudia Turro[‡]*

[‡]*Department of Chemistry and Biochemistry, The Ohio State University, Columbus, OH 43210*

[†]*Department of Chemistry, University of Houston, Houston, TX 77004*

Abstract. Two new complexes, [Ru(tpy)(qdppz)]$(PF_6)_2$ (**1**; qdppz = 2-(quinolin-8-yl)dipyrido[3,2-a:2',3'-c]phenazine, tpy = 2,2':6',2''-terpyridine) and [Ru(qdppz)$_2$]$(PF_6)_2$ (**2**), were investigated for their potential use as phototherapeutic agents through their ability to photosensitize the production of singlet oxygen, $^1O_2$, upon irradiation with visible light. The complexes exhibit strong Ru(dπ)→qdppz(π*) metal-to-ligand charge transfer (MLCT) absorption with maxima at 485 nm and 495 for **1** and **2** in acetone, respectively, red-shifted from the Ru(dπ)→tpy(π*) absorption at 470 nm observed for $[Ru(tpy)_2]^{2+}$ (**3**) in the same solvent. Complexes **1** and **3** are not luminescent at room temperature, but ^{3}MLCT emission is observed for **2** with maximum at 690 nm (λ_{exc} = 480 nm) in acetone. The lifetimes of the ^{3}MLCT states of **1** and **2** were measured using transient absorption spectroscopy to be ~9 ns and 310 ns in methanol, respectively at room temperature (λ_{exc} = 490 nm). The bite angle of the qdppz ligand is closer to octahedral geometry than that of tpy, resulting in the longer lifetime of **2** as compared to those of **1** and **3**. Arrhenius treatment of the temperature dependence of the luminescence results in similar activation energies, E_a, from the ^{3}MLCT to the ^{3}LF (ligand field) state for the two complexes, 2520 cm^{-1} in **1** and 2400 cm^{-1} in **2**. However, the pre-exponential factors differ by approximately two order of magnitude, 2.3 x 10^{13} s^{-1} for **1** and 1.4 x 10^{11} s^{-1} for **2**, which, together with differences in the Huang-Rhys factors, lead to markedly different ^{3}MLCT lifetimes. Although both **1** and **2** intercalate between the DNA bases, only **2** is able to photocleave DNA owing to its $^1O_2$ production upon irradiation with Φ_Δ = 0.69. The present work highlights the profound effect of ligand bite angle on electronic structure, providing guidelines for extending the lifetime of ^{3}MLCT Ru(II) complexes with tridentate ligands, a desired property for a number of applications.

*Corresponding Author: turro.1@osu.edu

Introduction

The excited state properties of ruthenium(II) polypyridyl complexes have been utilized across diverse fields for applications that include solar energy conversion,[1–3] bioimaging,[4,5] photoswitching,[6,7] and photodynamic therapy (PDT).[8–15] PDT agents are not toxic in the dark and must be activated by light to produce cytotoxic reactive oxygen species, such as $^1O_2$.[8–15] This method provides spatiotemporal control of the delivery and dose of the drug at the tumor site.[8–15] Therefore, photoactivation affords selectivity towards cancer that is not present in traditional cancer chemotherapeutics, such as cisplatin and related platinum complexes, which are thermally activated.[8–15] In order to efficiently produce $^1O_2$ for PDT, ruthenium(II) complexes must possess a long-lived excited-state, be stable in the dark, and should absorb low energy visible light for maximum tissue penetration.[16]

In contrast to the prototypical $[Ru(bpy)_3]^{2+}$ (bpy = 2,2′-bipyridine) and derivatives with bidentate chelation,[17–19] Ru(II) photosensitizers coordinated by tridentate ligands, such as tpy (2,2′:6′,2″-terpyridine), have been explored for their increased red light absorption and a more favorable geometry for the preparation of supramolecular linear arrays.[20,21] However, the development of these complexes for light-driven applications has been limited by their short excited state lifetimes. For example, the ^{3}MLCT (metal-to-ligand charge transfer) excited state lifetime, τ, of $[Ru(tpy)_2]^{2+}$ is only 250 ps in water at room temperature,[22] significantly shorter than that of $[Ru(bpy)_3]^{2+}$, 685 ns, and related complexes with bidentate ligands.[23,24] For this reason, there has been intense interest in the development of Ru(II) complexes with tridentate ligands featuring longer ^{3}MLCT lifetimes.[17–20,25–34]

One strategy used to increase the excited state lifetimes of the bis-tridentate Ru(II) complexes is expansion of the ligand's bite angle.[18,25] The 157° bite angle of tpy (Figure 1a) is smaller than the ideal 180° required for an octahedral geometry around the metal center,[26] resulting in a weaker ligand-field splitting and lower energy metal-centered, triplet ligand-field excited state (^{3}LF). The ^{3}LF state serves to deactivate the emissive ^{3}MLCT excited state in these complexes, such that increasing the energy of the former results in longer ^{3}MLCT lifetimes.[18,19,27] One

successful design was shown to be the addition of quinoline substituents to the 2- and 5-positions of the central pyridine ring to generate 2,6-di(quinoline-8-yl)pyridine (dqpy), since the quinoline groups serve to expand the bite angle to 179.6° in dqpy (structure shown in Figure 1a), leading to an emissive ^{3}MLCT excited state in $[Ru(dqpy)_2]^{2+}$ with a lifetime, τ, of 3.0 μs in ethanol/methanol at room temperature.[28] Similar lifetimes were reported for bis-tridentate complexes with substituted dqpy ligands, some with emission in the near-IR region.[29–31] The addition of carbon bridges between pyridine units also results in an expanded tridentate coordination structure with bite angle of 168°, leading to an emissive bis-tridentate Ru(II) complex with τ = 18 ns in acetonitrile at 298 K (Figure 1a; bzbpy).[27] This ligand was further improved through the addition of carbonyl groups and two methylene bridges, expanding the bite angle to 177.8° and increasing the lifetime to 3.3 μs in acetonitrile at 298 K (Figure 1a; L_{Ket}).[32] The same principle can be applied to other ligands, such as the addition of a quinoline group to the 2-position of phen (1,10-phenanthroline) to generate qphen (qphen = 2-(quinolin-8-yl)-1,10-phenanthroline; Figure 1a). $[(Ru(qphen)_2)](PF_6)_2$ exhibits a ^{1}MLCT absorption centered at 485 nm and an emissive ^{3}MLCT state with maximum at 712 nm and τ = 810 ns in methanol/ethanol at 298 K.[33]

In the DNA light-switch complexes *cis*–$[Ru(bpy)_2(dppz)]^{2+}$ (dppz = dipyrido[3,2-a:2',3'-c]phenazine) and in *cis*-$[Ru(phen)_2(dppz)]^{2+}$ (phen = 1,10-phenathroline), the extended π-system of the dppz ligand is able to intercalate between the DNA bases, making the complexes emissive and turning on their ability to produce $^1O_2$ upon irradiation, such that they are able to photocleave DNA.[35–38] The present work combines the introduction of a tridentate ligand with an expanded coordination cage together with presence of a dppz unit in $[Ru(tpy)(qdppz)](PF_6)_2$ (**1**; qdppz = 3-(quinolin-8-yl)dipyrido[3,2-a:2',3'-c]phenazine) and $[Ru(qdppz)_2](PF_6)_2$ (**2**); the molecular structures of **1** and **2** are schematically depicted in Figure 1b. The results for complexes **1** and **2** are compared to those for the parent complex $[Ru(tpy)_2](PF_6)_2$ (**3**).

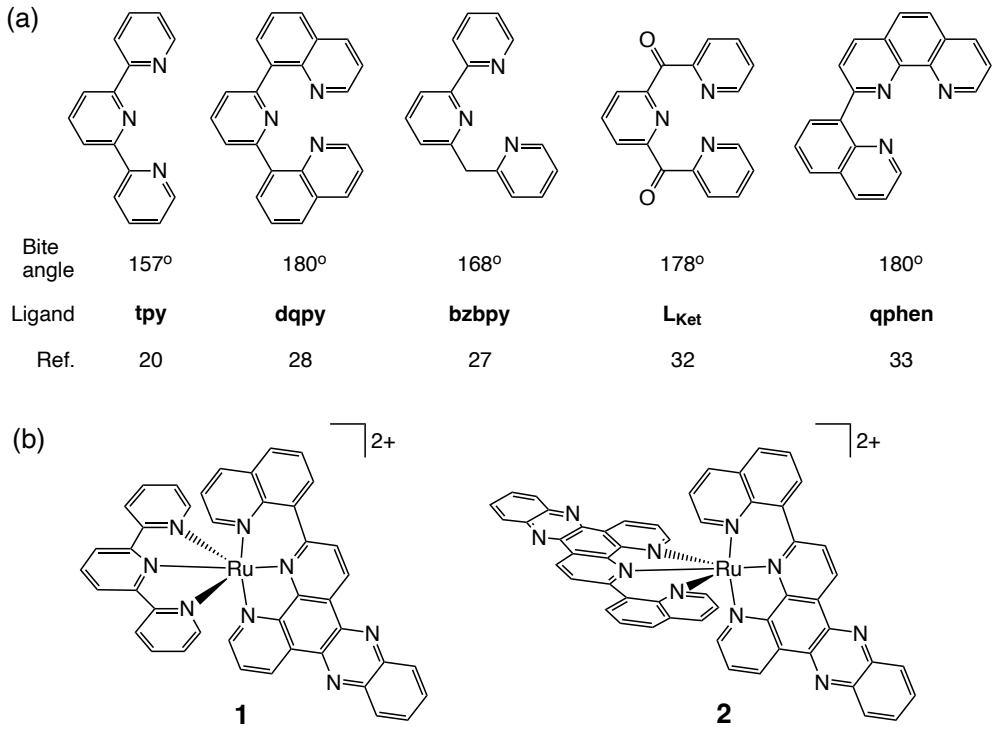

Figure 1. Structural representation of (a) tpy and related tridentate ligands with corresponding bite angles and (b) complexes **1** (left) and **2** (right).

Experimental

Materials. All materials were used as received without further purification unless otherwise noted. Diethyl ether, acetone, acetonitrile, and methanol were procured from Fisher Scientific, and dichloromethane was obtained from Macron Fine Chemicals. Additionally, 1,3-diphenylisobenzofuran (DPBF), 1,10-phenanthroline (phen), KPF_6 and acetone-d_6 were purchased from Sigma-Aldrich. $Ru(tpy)Cl_3$ was prepared using a known synthesis and the ligand qdppz was synthesized following modifications of published procedures as shown in Scheme SI and the process is described in detail in the supporting information, along with ^{1}H NMR characterization (Figures S1 – S3).[39–41]

[Ru(tpy)(qdppz)](PF$_6$)$_2$ (1). The ligand qdppz, 2-(quinolin-8-yl)dipyrido[3,2-a:2',3'-c]phenazine, was dissolved in 20 mL CH_2Cl_2:CH_3OH:H_2O (1:1:1, v:v:v) with $Ru(tpy)Cl_3$ and the reaction

mixture was refluxed overnight in the dark. The solution turned from purple to red and, after cooling to room temperature, the solvent was reduced under vacuum and the mixture was added dropwise to a saturated aqueous solution of KPF_6. The resulting precipitate was filtered and washed with water and diethyl ether. ^{1}H NMR (400 MHz; Figure S4) in $(CD_3)_2CO$, δ/ppm (mult., coupling, integration): 9.97 (d, J = 6.28 Hz, 1H), 9.90 (d, J = 6.28 Hz, 2H), 9.10 (d, J = 7.51 Hz, 2H), 8.78 (t, J = 8.42, Hz, 1H), 8.59-8.46 (m, 5H), 8.24 (d, J = 6.98, 1H), 7.87-7.80 (m, 3H),), 7.67-7.58 (m, 7H), 7.28 (d, J = 7.78 Hz, 1H) 7.10 (d, J = 7.34 Hz, 2H). ESI-TOF (+): $[M^{2+} - 2\ PF_6]^{2+}$ m/z = 372.08, $[M^{2+} -1\ PF_6]^{+}$ m/z = 889.16 (Figure S6).

$[Ru(qdppz)_2](PF_6)_2$ (2). Two equivalents of qdppz ligand (0.100 g, 0.354 mmol) were dissolved in 20 mL CH_2Cl_2:CH_3OH:H_2O (1:1:1, v:v:v) with $RuCl_3$ (0.0367 g, 0.177 mmol) and the same synthetic procedure was followed as that to prepare **1**. ^{1} H NMR (400 MHz) in $(CD_3)_2CO$, δ/ppm (mult., coupling, integration): 10.12 (d, J = 7.12 Hz, 2H), 9.51 (d, J = 6.28 Hz, 2H; Figure S5), 9.35 (dd, J = 6.28, 1.44 Hz, 2H), 9.18 (dd, J = 8.42, 1.48 Hz, 2H), 8.87 (d, J = 7.78, 1.39 Hz, 2H), 8.61 (dd, J = 8.44, 1.41 Hz, 2H), 8.41 (dd, J = 6.64, 1.41 Hz, 1H), 8.27-8.15 (m, 8H), 8.08–8.04 (m, 4H), 7.53 (td, J = 8.51, 1.44 Hz, 2H), 7.07 (td, J = 6.56, 1.48 Hz, 1H). ESI-TOF (+): $[M^{2+} - 2\ PF_6]^{2+}$ m/z = 460.08 , $[M^{2+} -1\ PF_6]^{+}$ m/z = 1065.13 (Figure S6).

Instrumentation and Methods. ^{1}H spectra were measured on a Bruker 400 MHz DPX spectrometer. The ^{1}H-NMR peaks were referenced to the residual protonated acetone solvent at 2.05 ppm. Electrospray ionization (ESI) mass spectrometry was conducted on a Bruker MicroTOF spectrometer. Samples were dissolved in acetonitrile. Electronic absorption spectra were recorded on a Hewlett Packard 8453 diode array spectrometer, and emission spectra were collected on a Horiba Fluormax-4 Fluorimeter.

Franck-Condon line shape analysis (eq 1) was used to fit the 77 K emission spectrum of each complex with Wolfram Mathematica using the Levenberg – Marquardt procedure.[42] The four parameters that are fitted through this analysis are E_{00}, the energy difference between the lowest energy vibrational level of the emissive excited state and that of the ground state, S_m, the Huang-

Rhys factor which provides a quantitative measure of the relative distortion between the states, $\hbar\omega$ corresponds to the energy of the ground state acceptor vibrational mode, and $\Delta\nu_{1/2}$ is the full-width

$$I(\tilde{\nu}) = \sum_{\nu_m}^{\infty} \left\{ \left(\frac{E_{00} - \nu_m \hbar\omega}{E_{00}} \right)^3 \left(\frac{S_m{}^{\nu_m}}{\nu_m!} \right) \exp \left[\frac{(\tilde{\nu} - E_{00} + \nu_m \hbar\omega)^2}{\Delta\nu_{1/2}} \right] \right\} \quad (1)$$

at half maximum.[42] In eq 2, ν_m represents the number of vibronic modes used in the fit, varied from $\nu_m = 0$ to $\nu_m = 2$; in cases where the fit was not satisfactory, the sum included $\nu_m = 3$.

The quantum yields for $^1O_2$ production (Φ_Δ) were measured using $[Ru(bpy)_3]^{2+}$ as a standard with $\Phi_\Delta = 0.81$ in CH_3OH,[43] and DPBF as a $^1O_2$ trap. The absorbance of the unknown samples and that of the $[Ru(bpy)_3]^{2+}$ standard were matched at the irradiation wavelength (A = 0.01 at 460 nm) in a 1×1 cm quartz cuvette in methanol. The samples were irradiated in the sample compartment of the fluorimeter (λ_{irr} = 460 nm) in the presence of 1.0 μM DPBF. The DPBF emission intensity (λ_{ex} = 405 nm; λ_{em} = 479 nm) was plotted as a function of irradiation time. The resulting data points fit linear relationship, and the quantum yield was determined by comparing the resulting slopes for the sample with that for the $[Ru(bpy)_3]^{2+}$ standard.

Determination of the DNA binding constants was carried out through monitoring the change of the ^{1}MLCT absorption of each complex upon the addition of calf thymus DNA, which can be correlated to the DNA binding constant (K_b) using eq 2, where ε_a, ε_f, and ε_b correspond to the extinction coefficient for the apparent, free, and bound ruthenium complex, respectively, $b = 1 + K_bC_t + K_b[DNA]_t/2s$, where C_t and $[DNA]_t$ represent the total complex and total DNA concentrations, respectively, and *s* is the base pair binding site size.[44,45]

$$\frac{(\varepsilon_a - \varepsilon_f)}{(\varepsilon_b - \varepsilon_f)} = \frac{2 - (b^2 - 2K_b^2 C_t [DNA]_t/s)^{1/2}}{2K_b C_t} \quad (2)$$

DNA photocleavage experiments were carried out with 20 μL total volume in transparent 0.5 mL Eppendorf tubes containing 100 μM pUC19 plasmid (concentration in bases), 10 or 20 μM of each complex, and 5 mM Tris buffer (pH = 7.7, 50 mM NaCl) in water. After incubation for 30

minutes in the dark at room temperature, the samples were irradiated with a 150 W Xe arc lamp ($\lambda_{irr} \geq 395$ mn). After irradiation, 4 μL of loading dye buffer was added to each sample. The solutions were loaded into a 1% agarose gel (stained with 0.5 μg/mL ethidium bromide) in a 1X TAE buffer (40 mM Tris-acetate, 1 mM EDTA, pH ~8.5). Gel electrophoresis was performed at a voltage of 60 V for ~1.5 hours and the gels were imaged using a BioRad GelDoc 2000 transilluminator.

For nanosecond transient absorption (nsTA) experiments, the excitation source was an optical parametric oscillator (basiScan, Spectra-Physics) pumped by an Nd:YAG laser (Quanta-Ray INDI, Spectra-Physics) with fwhm ~ 6 ns at a repetition rate of 10 Hz. The spectrometer (LP980, Edinburgh Instruments) used a continuous 150 W xenon arc lamp as a probe source. The spectral measurements were collected with an ICCD camera, while the kinetic traces were measured with a PMT and a digital oscilloscope at a single wavelength. Samples for nsTA were prepared in a 1×1 cm quartz cuvette with an absorbance of ~0.5 at the excitation wavelength. The temperature dependence of the luminescence was collected using a CoolSpeK UV USP-203-B cryostat (UNISOKU Scientific Instruments) to achieve temperatures ranging from 173 K to 298 K. The resulting values where then fitted to the Arrhenius equation (eq 3), where E_a is the activation energy, A the pre-exponential factor, and k_o the sum of the non-radiative and radiative decay rate constants.

$$\frac{1}{\tau} = k_o + A \exp\left(-\frac{E_a}{k_b T}\right) \quad (3)$$

Results and Discussion

Steady-State Photophysical Properties

The electronic absorption spectra of **1** and **2** are shown in Figure 2. Both complexes exhibit a strong dppz-centered $^1\pi\pi^*$ transition at ~360 nm in acetone, with ε = 43,700 $M^{-1}cm^{-1}$ for **1** and ε = 75,900 $M^{-1}cm^{-1}$ for **2**. These maxima for **1** and **2** are similar to that reported for

$[Ru(bpy)_2(dppz)]^{2+}$ at 372 nm in water.[44] Compared to the ^{1}MLCT absorption of $[Ru(tpy)_2]^{2+}$ at 470 nm in acetone,[22] the absorption maxima are slightly red-shifted, observed at 485 nm for **1** and 495 nm for **2** in acetone. These values are consistent with those previously reported for the related complexes $[Ru(tpy)(pydppz)]^{2+}$ (pydppz = 3-(pyrid-2'-yl)dipyrido[3,2-a:2',3'-c]phenazine) and $[Ru(pydppz)_2]^{2+}$, with ^{1}MLCT absorption maxima at 476 and 475 nm in CH_3CN, respectively.[46]

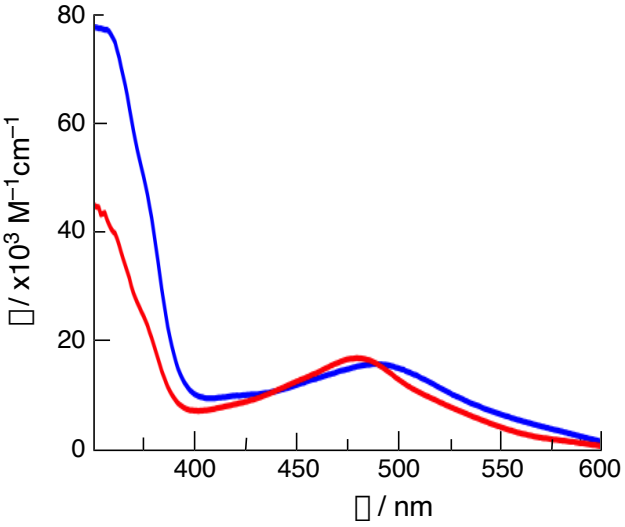

Figure 2. Electronic absorption spectra of **1** (red) and **2** (blue) in acetone at 298 K.

Although luminescence was not observed for **1** at room temperature in CH_3CN, **2** was emissive at 298 K in the same solvent with a maximum at 690 nm, as shown in Figure 3a. Excitation of **1** and **2** with 490 nm light at 77 K in CH_3CN results in a broad emission with maxima at 677 nm and 700 nm, respectively (Figure 3b). The 77 K emission spectra of each complex also exhibit a lower intensity shoulder at ~750 nm, which corresponds to a vibronic progression with an energy separation of ~1200 cm^{-1} from the E_{00} maximum. This value is comparable to that reported for the low temperature luminescence of $[Ru(tpy)_2]^{2+}$, 1290 cm^{-1}.[21,33]

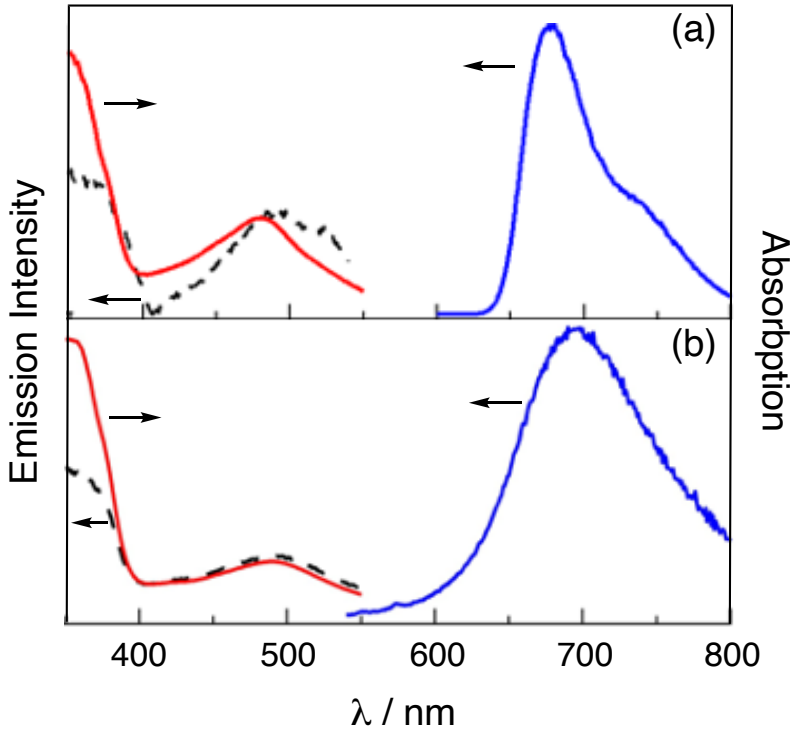

Figure 3. Emission (blue solid line; λ_{exc} = 490 nm), absorption (red, solid line; 298 K), and excitation (black, dashed line; λ_{em} = 675 nm) of (a) **1** at 77 K (b) **2** at 298 K in CH_3CN under N_2.

Time-Resolved Optical Measurements

The excited state dynamics of **1** and **2** were investigated using nanosecond transient absorption (nsTA) spectroscopy in deaerated methanol (λ_{ex} = 490 nm, IRF ~ 6 ns). It is evident from Figure 4 that both complexes exhibit similar positive transient absorption features at ~400 nm and ground state bleach signals from 450 nm to 600 nm. In addition, the TA spectrum of **2** exhibits a broad, weaker positive absorption at ~650 nm that is not observed for **1**, possibly due to a lower signal-to-noise ratio in the spectra of the latter. The transient signals of **2** at 400 nm and 650 nm can be fitted to monoexponential decays with a lifetime τ = 310 ns in methanol (Table 1). A similar lifetime is obtained for the bleach recovery of **2** measured at 490 nm, τ = 315 ns. The lifetime of **1** is significantly shorter, τ ~ 9 ns for both the positive TA signal at ~400 nm and the bleach at 490 nm. It should be noted that similar kinetics are observed in **1** and **2** for the decay of

the positive transient signal at ~400 nm and the return of the bleach is consistent with the decay of ^{3}MLCT directly back to the ground state, as is typical for Ru(II) polypyridyl complexes.[47–49] Additionally, the emission lifetime for **2**, was measured to be 318 ns under N_2 in CH_3OH (λ_{exc} = 355 nm, λ_{em} = 675 nm), consistent with the nsTA results.

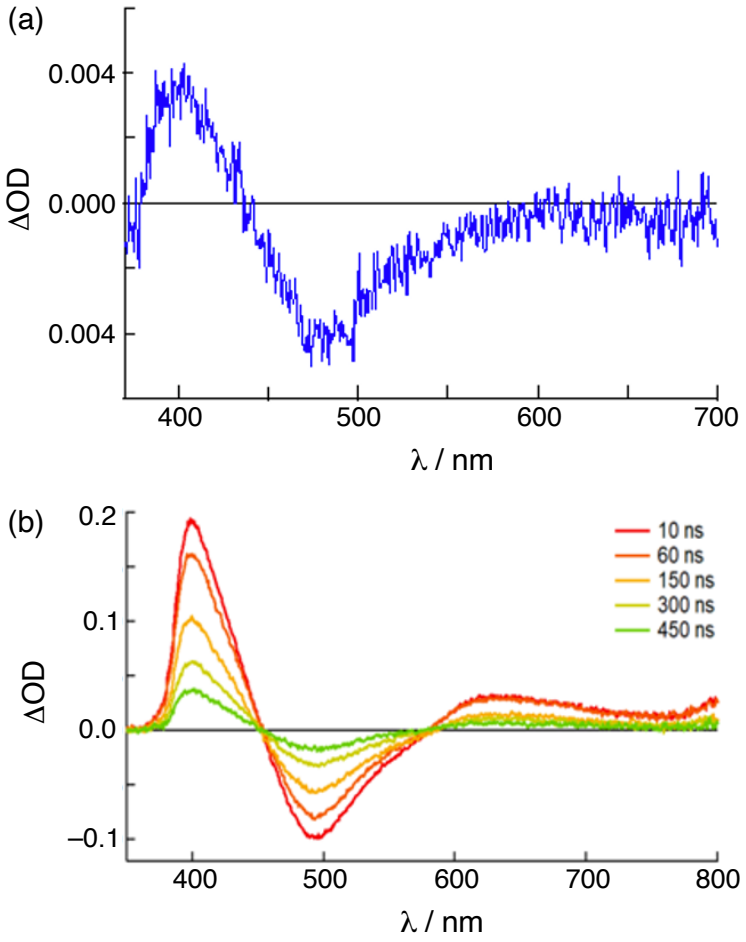

Figure 4. Transient absorption spectra of (a) **1** recorded 5 ns after the excitation pulse and (b) **2** collected 10 ns to 450 ns following excitation in deaerated CH_3OH (λ_{exc} = 490 nm).

The difference in the excited state lifetimes of **1** and **2** parallel those previously reported for Ru(II) heteroleptic and homoleptic complexes with tridentate ligands. For example, the ^{3}MLCT lifetime of $[Ru(2\text{-pybpy})_2]^{2+}$ (pybpy = 6-(pyridine-2-ylmethyl)-2,2'-bipyridine) was reported to be 15 ns at room temperature in acetonitrile, a ~10-fold increase when compared to the 1.4 ns lifetime

of [Ru(ttpy)(2-pybpy)]$^{2+}$ (ttpy = 4′-tolyl-2,2′:6′,2″-terpyridine) under similar experimental conditions; the latter is coordinated by a substituted tpy ligand, ttpy, with a bite angle that deviates from the ideal octahedral geometry.[18]

Table 1. Excited State Lifetimes, τ, Activation Energies, E_a, and Pre-exponential Factors, A, from Arrhenius Fits of the Temperature Dependence of the Emission Lifetimes, and Franck-Condon Analysis Values for **1** – **3**.

Complex	τ / ns [a]	E_a / cm^{-1} [b]	A / s^{-1} [b]	E_{00} / cm^{-1}	$\hbar\omega$ / cm^{-1}	S_m	$\Delta\nu_{1/2}$ / cm^{-1}
1	~9	2520	2.3×10^{13}	14700	1130	0.58	1000
2	310	2400	1.4×10^{11}	14770	1120	0.80	1120
3	0.25[d]	1700[e]	1.7×10^{13}[e]	17100[e,f]	1380[e,f]	0.43[e,f]	750[e,f]

[a]Methanol, 298 K, under N_2. [b]In acetone. [d]Data from ref. 50 in water, 298 K. [e]Data from ref. 51 in butyronitrile. [f]At 77 K.

Temperature Dependence Studies

To further understand the differences in the excited state processes in **1** and **2**, the temperature dependence of their luminescence lifetimes was investigated. In particular, the shorter lifetime of **1**, as is the case in other tpy Ru(II) complexes, may be related to the lower energy of the ^{3}LF state associated with the reduced bite angle of the tpy ligand as compared to those of the two qdppz ligands in **2**. The ^{3}MLCT lifetimes for **1** and **2** were measured from 173 K to 333 K in acetone, shown in Figure S7, and fitted with Eq 3 at a probe wavelength of 715 nm. The resulting values of the activation energy, E_a, and pre-exponential factor, A, are listed in Table 1. Both complexes exhibit an increase in lifetime as the temperature, T, is decreased, however, the temperature at which the lifetime reaches a limiting value differs. The emission lifetime of **1** generally varies across the entire temperature range, in contrast to the behavior observed for **2**,

which exhibits relatively constant lifetimes at T < 240 K (Figure 5). The Arrhenius fits resulted in similar energy barriers for the two complexes, E_a = 2520 cm^{-1} for **1** and E_a = 2400 cm^{-1} for **2**. These values are within the range previously reported in the literature for emissive Ru(II) complexes, including $[Ru(tpy)_2]^{2+}$ with E_a = 1700 cm^{-1} and $[Ru(bpy)_3]^{2+}$ with E_a = 3960 cm^{-1}.[24,51] The lower E_a value for $[Ru(tpy)_2]^{2+}$ as compared to $[Ru(bpy)_3]^{2+}$ is attributed to a greater distortion from octahedral geometry around the metal in the former, resulting in a lower energy ^{3}LF state than in $[Ru(bpy)_3]^{2+}$.[51]

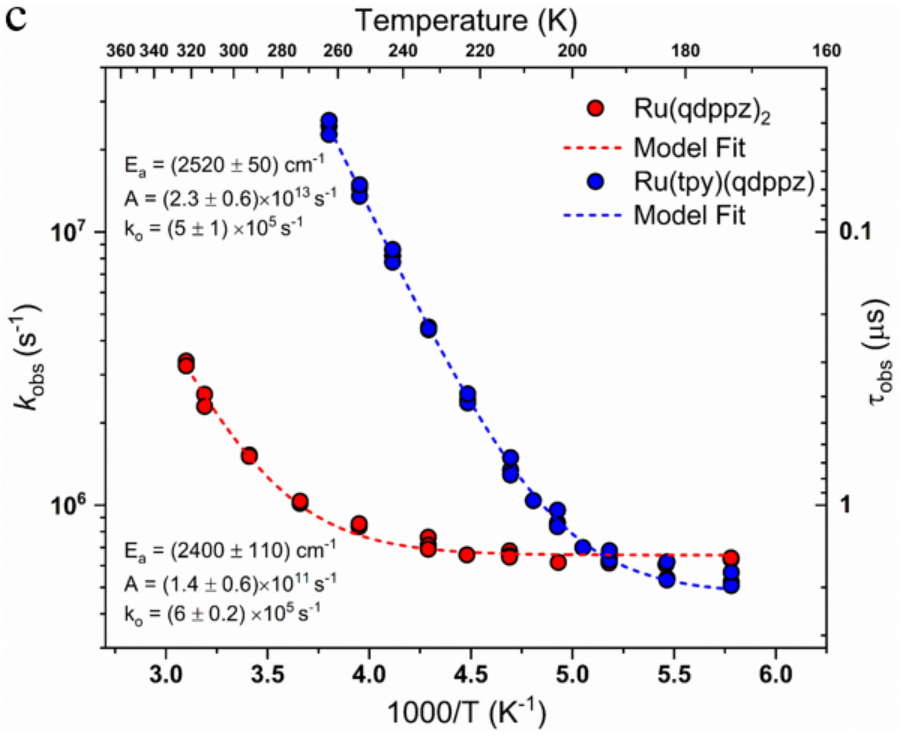

Figure 5. Temperature dependence of the measured k_{obs} (= $1/\tau_{obs}$), obtained from the luminescence lifetimes, τ_{obs}, of **1** (blue) and **2** (red) along with the corresponding fits (dashed lines) in acetone (λ_{ex} = 532 nm).

Since the ^{3}MLCT to ^{3}LF energy barriers E_a are nearly identical in **1** and **2**, the pronounced difference in the lifetimes between the complexes may be attributed to the pre-exponential frequency factor A. The Arrhenius fit for complex **1** resulted in A = 2.3 × 10^{13} s^{-1}, two orders of magnitude greater than that for **2**, A = 1.4 × 10^{11} s^{-1}. The difference in pre-exponential factors

between these two complexes can be explained by the presence of distinct pathways for deactivation through the ^{3}LF state, as shown in Figure 6.[24] In Case I, deactivation from the ^{3}LF to the ^{1}GS state, which is determined by k_2, is significantly faster than the reverse crossing from the ^{3}LF back to the ^{3}MLCT, k_{-1}, such that $k_2 >> k_{-1}$.[24,52] This case is the most common for Ru(II) complexes, including $[Ru(tpy)_2]^{2+}$ ($A = 1.7\times10^{13}$ s^{-1}, $E_a = 1700$ cm^{-1})[51] and $[Ru(bpy)_3]^{2+}$ ($A = 1.3\times10^{14}$ s^{-1}, $E_a = 3960$ cm^{-1}),[24] both with pre-exponential factors in the vibrational frequency range, $10^{12} - 10^{14}$ s^{-1}. In contrast, in Case II, the return to the ^{3}MLCT state from the ^{3}LF, k_{-1}, competes with the deactivation through the ^{3}LF state, such that $k_{-1} \sim k_2$, allowing the ^{3}MLCT and ^{3}LF to equilibrate, resulting in pre-exponential factors in the range of $10^9 - 10^{10}$ s^{-1}.[19,53,54] Case II appears to be rare, with only a few reports of tridentate ruthenium(II) complexes that exhibit this behavior.[33,52] It is clear from the pre-exponential factors in Table 1 that **1** falls within Case I, similar to that of $[Ru(tpy)_2]^{2+}$ and $[Ru(bpy)_3]^{2+}$, whereas complex **2** is among the few examples that follow the kinetic scheme of Case II. The fast deactivation through the ^{3}LF state for **1** also serves to explain its significantly shorter ^{3}MLCT lifetime as compared to **2**.

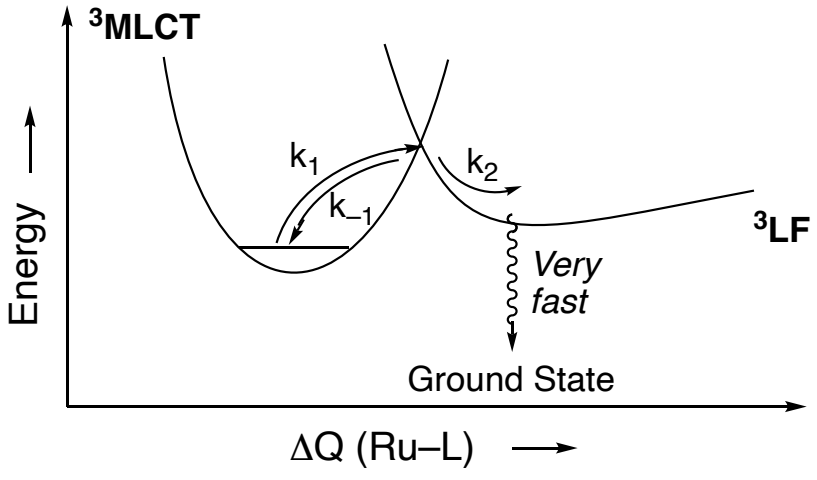

Figure 6. Diagram showing the deactivation of the ^{3}MLCT excited state through the ^{3}LF state where in Case I, $k_2 >> k_{-1}$ and in Case II, where k_{-1} competes with k_2.

Franck-Condon line shape analysis of the 77 K emission spectra of **1** and **2** was performed using eq 1 and the resulting fits are shown in Figure S8. The values of E_{00}, the energy difference between the lowest energy vibrational levels of the ground state (^{1}GS) and the emissive ^{3}MLCT excited state, S_m, the Huang-Rhys factor that provides a quantitative measure of the distortion in the ^{3}MLCT relative to the ^{1}GS, $\hbar\omega$, which corresponds to the ground state acceptor vibrational mode, and $\Delta\nu_{1/2}$, the full-width at half maximum, were obtained from the fits and are listed in Table 1. The fits for **1** and **2** result in similar $\hbar\omega$ and E_{00} values, ~1130 cm^{-1} and ~14700 cm^{-1}, respectively, and parallel those reported for **3**, $[Ru(tpy)_2]^{2+}$, 1380 cm^{-1} and 17100 cm^{-1} at 77 K in buryronitrile.[51] The E_{00} value from these fits is in good agreement with that obtained from the steady state emission of **1** and **2** at 77 K, ~14500 cm^{-1} (Figure S8). The difference between the values for **1** and **2** compared to that of **3** can be explained by the addition of the qdppz ligand, which not only extends conjugation but also increases the bite angle of the ligand. Despite similar $\hbar\omega$ and E_{00} values, $S_m = 0.58$ was determined for **1** and $S_m = 0.80$ for **2**. For comparison, fits of the 77 K emission of $[Ru(tpy)_2]^{2+}$ and $[Ru(bpy)_3]^{2+}$ result in S_m values of 0.41 and 0.95, respectively.[42b,51]

S_m is related to the change in equilibrium displacement (ΔQ_e), frequency (ω), and the reduced mass (M) by the equation $S_m = (1/2)(M\omega/h)(\Delta Q_e)^2$.[55,56] Therefore, with similar ω and M in **1** and **2**, a smaller S_m value indicates a smaller amount of relative distortion between the ^{3}MLCT state and the ^{1}GS in **1** as compared to **2** (Table 1), as schematically depicted in Figure 7.[55,56] In addition to the displacement between the ^{3}MLCT and ^{1}GS states, Figure 7 provides a representation for the potential energy surfaces of **1** and **2** based on their similar E_{00} and E_a values, together with the lower energy of the ^{3}LF state for **1** relative to **2** afforded by the smaller bite angle of the former. The Huang-Rhys value for **1** is similar to that of **3**, and that observed for **2** is in good agreement with a previously reported value for $[Ru(dqp)_2]^{2+}$ (dqp = 2,6-di(quinolin-8-yl)pyridine), $S_m = 0.99$, believed to arise from the deviation from planarity of the dqp ligand in the ground state.[19,28] Interestingly, Arrhenius treatment of the emission of $[Ru(dqp)_2]^{2+}$ resulted in a pre-

exponential factor of 1.5×10^{10} s^{-1}, placing it Case II along with complex **2**, and providing an additional example of similarity in the photophysical properties between these two compounds.[19]

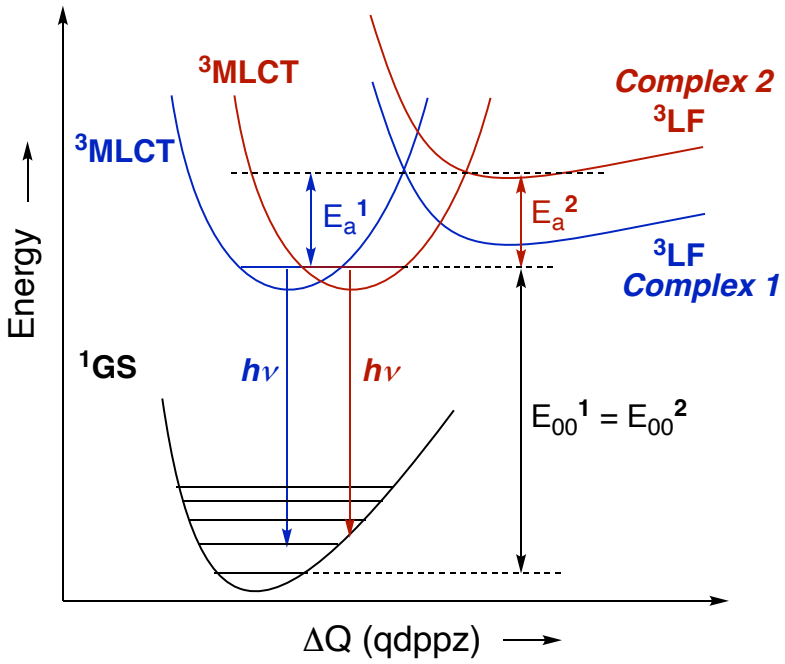

Figure 7. Schematic representation of the relative energies and displacements of the potential energy surfaces of **1** and **2**.

DNA Binding and Photocleavage

The ability of **1** and **2** to photocleave plasmid DNA was assessed using agarose gel electrophoresis with 90 μM pUC19 DNA bases (5 μM Tris, pH = 7.6, 50 μM NaCl), as shown in Figure 8. In Figure 8, lanes 1 and 6 contain plasmid alone showing mostly form I (undamaged, supercoiled) and a smaller amount of form II (single-strand cleavage, open circular) DNA. Lanes 2 and 3 contain 15 μM of **1** and lanes 4 and 6 15 μM of **2**; in lanes 2 and 4 the plasmid was incubated with each complex at room temperature in the dark for 15 min, and lanes 3 and 5 were irradiated for 15 min ($\lambda_{irr} \geq 395$ mn). In the presence of **1,** neither lane 2 (dark) nor the irradiated sample (lane 3) show DNA photocleavage. However, in the presence of **2**, DNA photoleavage is

observed upon irradiation (lane 5), but not when the sample is kept in the dark (lane 4). The photocleavage by **2** is attributed to its ability to sensitize the production of $^1O_2$, with quantum yield for $^1O_2$ production measured to be 0.69(2) in methanol under N_2 (λ_{irr} = 460 nm). In contrast, the sensitization of singlet oxygen was not observed for **1** under similar irradiation conditions, consistent with its short excited state lifetime and lack of photoreactivity towards the plasmid. The photoinduced generation of $^1O_2$ is known induce DNA damage through guanine oxidation to form 8-oxo-guanine,[57,58] however, strong association of the sensitizer with DNA is necessary for photocleavage to be observed.[59]

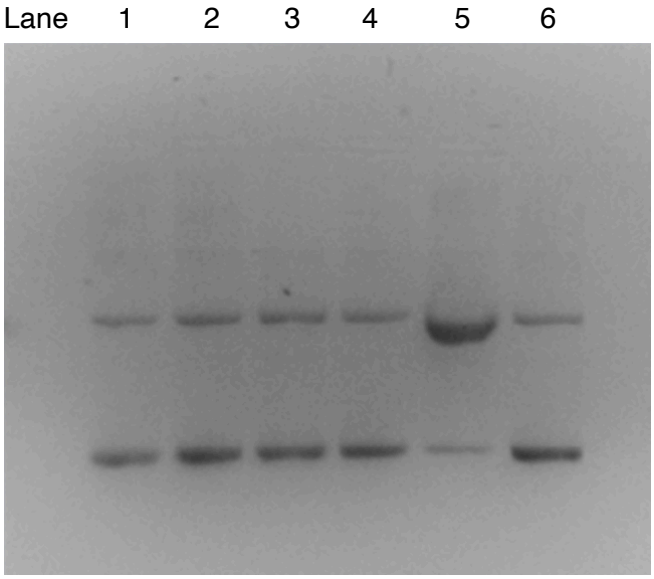

Figure 8. Ethidium bromide-stained agarose gel (1%) with 90 μM pUC19 (bases), 5 mM Tris buffer (pH = 7.6), 50 mM NaCl. Lanes 1 and 6 contain plasmid only, lanes 2 and 3 15 μM of **1**, and lanes 4 and 5 15 μM of **2**. Lanes 3 and 5 were irradiated ($\lambda_{irr} \geq$ 395nm, 15 min) and lanes 2 and 4 were kept in the dark for 15 min.

The DNA binding constant, K_b, of each complex was determined by monitoring the changes in the electronic absorption spectra of 15 mM **1** and **2** upon addition of up to 100 μM calf-thymus DNA bases (5 mM Tris, pH 7.1, 50 mM NaCl). The absorption changes were fit to a previously reported 1:1 binding model (eq 2) that includes the binding site size, *s*.[44,60,61] The bathochromic shifts of the absorption of **1** and **2** at 490 nm resulted in DNA K_b values of 5.7×10^5

M^{-1} (s = 2.8) for **1** and 5.4 × 10^5 M^{-1} (s = 3.0) for **2** (Figure S9). These values are consistent with those reported for cationic transition metal intercalators, including those with dppz ligands, such as $[Ru(phen)_2(dppz)]^{2+}$ with K_b = 1 × 10^6 M^{-1} (s = 2).[60,61]

Relative viscosity measurements were performed to provide additional evidence of intercalation by each complex, as previously reported for transition metal complexes with a dppz ligand.[62,63] Figure 9 shows the changes in the relative viscosity of a 200 μM calf thymus DNA solution (5 mM Tris buffer, 50 mM NaCl, pH = 7.0) upon addition of **1** and **2**, as well as with the known intercalator ethidium bromide (EtBr) and $[Ru(bpy)_3]^{2+}$, a complex that does not intercalate and exhibits weak electrostatic interactions with the DNA polyanionic backbone.[45,64–66] It is evident from Figure 9 that the addition of **1** and **2** results in an increase of the relative viscosity of the solution, similar to the results observed for EtBr. As expected, little change in the relative viscosity is recorded upon the addition of $[Ru(bpy)_3]^{2+}$. These results are consistent with DNA intercalation by **1** and **2** and show that the addition of the quinoline arm to the dppz ligand in qdppz does not affect the ability of the complexes to intercalate between the DNA bases.

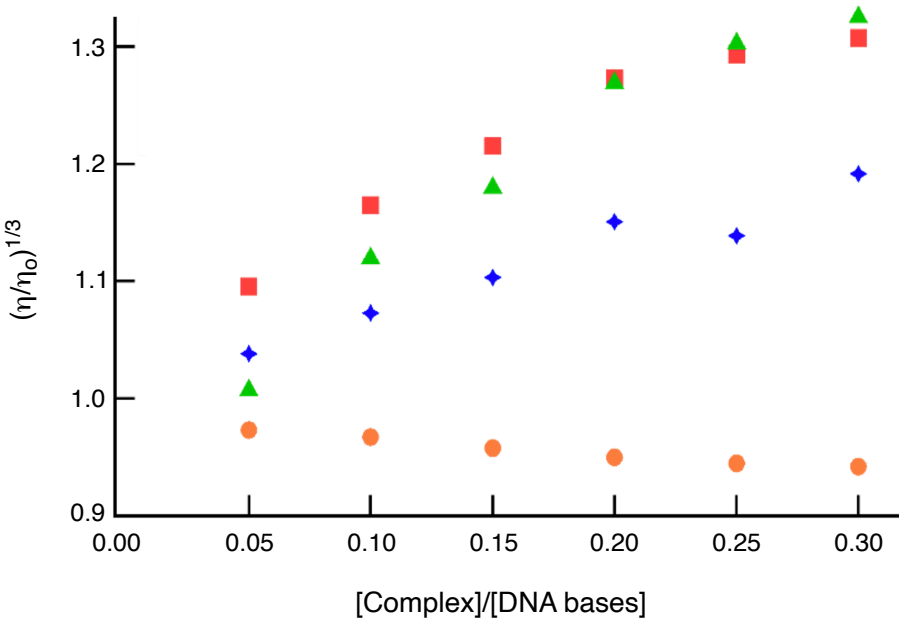

Figure 9. Relative viscosity of 200 μM calf thymus DNA (bases, 5 mM Tris buffer, pH = 7.0, 50 mM NaCl) as a function of increasing concentration of EtBr (■), **1** (✦), **2** (▲), and $[Ru(bpy)_3]^{2+}$ (●).

Conclusion

The photophysical properties to two new complexes, $[Ru(tpy)(qdppz)](PF_6)_2$ (**1**) and $[Ru(qdppz)_2](PF_6)_2$ (**2**), were characterized. Complexes **1** and **2** feature strong ^{1}MLCT absorption in the visible region with maxima at ~490 nm. The presence of the tpy ligand in **1** aids in the deactivation of the ^{3}MLCT excited state through lowering the energy of the metal-centered ^{3}LF state, resulting in a ^{3}MLCT lifetime of ~9 ns at room temperature. In contrast, the larger bite angle of the qdppz ligands in **2** lead to a longer lifetime, 310 ns in methanol at 298 K. Arrhenius treatment of the temperature dependence of the ^{3}MLCT emission of **1** and **2** show that the differences in the excited state lifetimes of the complexes cannot be attributed to the energy barrier between the emissive ^{3}MLCT state and the ^{3}LF. Instead, Franck-Condon analysis of the 77 K emission of **1** and **2** point to increased distortion of the ^{3}MLCT excited state relative to the ground state in **2** compared to **1**, resulting in the longer lifetime of the former. Complex **2** is able to sensitize the generation of $^1O_2$ upon irradiation with $\Phi_\Delta = 0.69$, whereas the short excited state lifetime of **1** precludes bimolecular energy transfer to O_2. Both **1** and **2** intercalate between the DNA bases, however, only complex **2** is able to photocleave DNA through the production of $^1O_2$. Overall, the qdppz ligand in $[Ru(qdppz)_2]^{2+}$, **2**, represents a new example of a tridentate coordination to Ru(II) that affords long excited state lifetimes, making it potentially useful for a number of applications, including serving a s building block for linear arrays.

Supporting Information. Synthetic procedures; ^{1}H NMR and mass spectrometry characterization; emission decays as a function of temperature; emission spectra and Franck-Condon fits; DNA binding titration (PDF).

Acknowledgments. The authors thank the National Science Foundation (CHE-2102508) for partial support of this work .

References

(1) Turlington, M. D.; Brady, M. D.; Meyer, G. J. Dual-Sensitizer Photoanode for Bromide Oxidation. *ACS Appl. Entergy Mat.* **2021**, *4*, 745–754.

(2) Meyer, T. J.; Sheridan, M. V.; Sherman, B. D. Mechanisms of Molecular Water Oxidation in Solution and Oxide Surfaces. *Chem. Soc. Rev.* **2017**, *46*, 6148-6169.

(3) Aghazada, S.; Nazeeruddin, M. K. Ruthenium Complexes as Sensitizers in Dye-Sensitized Solar Cells. *Inorganics* **2018**, *6*, 52.

(4) Shum, J.; Leung, P. K.; Lo, K. K. Luminescent Ruthenium(II) Polypyridine Complexes for a Wide Variety of Biomolecular and Cellular Applications. *Inorg. Chem.* **2019**, *58*, 2231–2247.

(5) Li, J. J.; Guo, L.; Tian, Z.; Zhang, S.; Xu, Z.; Han, Y.; Li, R.; Li, Y.; Liu, Z. Half-Sandwich Iridium and Ruthenium Complexes: Effective Tracking in Cells and Anticancer Studies. *Inorg. Chem.* **2018**, *57*, 13552–13563.

(6) McClure, B. A.; Abrams, E. R.; Rack, J. J. Excited State Distortion in Photochromic Ruthenium Sulfoxide Complexes. *J. Am. Chem. Soc.* **2010**, *132*, 5428–5436.

(7) Sundin, E.; Johansson, F.; Saavedra Becerril, V.; Wallenstein, J.; Gasslander, A.; Mårtensson, J.; Abrahamsson, M. Two-Colour Photoswitching in Photoresponsive Inorganic Thin Films. *Mater. Adv.* **2021**, *2*, 2328–2333

(8) Kuang, S.; Wei, F.; Karges, J.; Ke, L.; Xiong, K.; Liao, X.; Gasser, G.; Ji, L.; Chao, H. Photodecaging of a Mitochondria-Localized Iridium(III) Endoperoxide Complex for Two-Photon Photoactivated Therapy under Hypoxia. *J. Am. Chem. Soc.* **2022**, *144*, 4091–4101.

(9) DeRosa, M. C.; Crutchley, R. J. Photosensitized Singlet Oxygen and Its Applications. *Coord. Chem. Rev.* **2002**, *233–234*, 351–371.

(10) Knoll, J. D.; Turro, C. Control and Utilization of Ruthenium and Rhodium Metal Complex Excited States for Photoactivated Cancer Therapy. *Coord. Chem. Rev.* **2015**, *282–283*, 110–126.

(11) Shi, G.; Monro, S.; Hennigar, R.; Colpitts, J.; Fong, J.; Kasimova, K.; Yin, H.; DeCoste, R.; Spencer, C.; Chamberlain, L.; et al. Ru(II) Dyads Derived from α-Oligothiophenes: A New Class of Potent and Versatile Photosensitizers for PDT. *Coord. Chem. Rev.* **2015**, *282–283*, 127–138.

(12) Zeng, L.; Gupta, P.; Chen, Y.; Wang, E.; Ji, L.; Chao, H.; Chen, Z.-S. The Development of Anticancer Ruthenium(II) Complexes: From Single Molecule Compounds to Nanomaterials. *Chem. Soc. Rev.* **2017**, *46*, 5771–5804.

(13) Chettri, A.; Cole, H. D.; Iii, J. A. R.; Schneider, K. R. A.; Yang, T.; Cameron, C. G.; Mcfarland, S. A.; Dietzek-ivans, B. Interaction with a Biomolecule Facilitates the Formation of the Function-Determining Long-Lived Triplet State in a Ruthenium Complex for Photodynamic Therapy. *J. Phys. Chem. A* **2022**, *126*, 1336–1344.

(14) Liang, R.; Xiong, W.; Lo, K. C.; Ho, P. Y.; Bai, X.; Lai, W.; Chan, W. K.; Du, L.; Phillips, D. L. Revealing the Photophysical Dynamics of Selected Rigid Donor − Acceptor Systems: From Ligands to Ruthenium(II) Complexes. *J. Phys. Chemisytry Lett.* **2021**, *12*, 10927–10935.

(15) Paul, S.; Kundu, P.; Kondaiah, P.; Chakravarty, A. R. BODIPY-Ruthenium(II) Bis-Terpyridine Complexes for Cellular Imaging and Type-I/-II Photodynamic Therapy. *Inorg. Chem.* **2021**, *60*, 16178–16193.

(16) Monro, S.; Colón, K. L.; Yin, H.; Roque, J.; Konda, P.; Gujar, S.; Thummel, R. P.; Lilge, L.; Cameron, C. G.; McFarland, S. A. Transition Metal Complexes and Photodynamic Therapy from a Tumor-Centered Approach: Challenges, Opportunities, and Highlights from the Development of TLD1433. *Chem. Rev.* **2019**, *119*, 797–828.
(17) Medlycott, E. A.; Hanan, G. S. Designing Tridentate Ligands for Ruthenium(II) Complexes with Prolonged Room Temperature Luminescence Lifetimes. *Chem. Soc. Rev.* **2005**, *34*, 133.
(18) Juris, A.; Balzani, V.; Barigelletti, F.; Campagna, S.; Belser, P.; Von Zelewsky, A. Ru(II) Polypyridine Complexes: Photophysics, Electrochemistry, and Chemiluminescence. *Coord. Chem. Rev.* **1988**, *84*, 85–277.
(19) Abrahamsson, M.; Becker, H. C.; Hammarström, L. Microsecond ^{3}MLCT Excited State Lifetimes in Bis-Tridentate Ru(II)-Complexes: Significant Reductions of Non-Radiative Rate Constants. *Dalton Trans.* **2017**, *46*, 13314–13321.
(20) Hammarström, L.; Johansson, O. Expanded Bite Angles in Tridentate Ligands. Improving the Photophysical Properties in Bistridentate Ru^{II} Polypyridine Complexes. *Coord. Chem. Rev.* **2010**, *254*, 2546–2559.
(21) Sauvage, J. P.; Collin, J. P.; Chambron, J. C.; Guillerez, S.; Coudret, C.; Balzani, V.; Barigelletti, F.; De Cola, L.; Flamigni, L. Ruthenium(II) and Osmium(II) Bis(Terpyridine) Complexes in Covalently-Linked Multicomponent Systems: Synthesis, Electrochemical Behavior, Absorption Spectra, and Photochemical and Photophysical Properties. *Chem. Rev.* **1994**, *94*, 993–1019.
(22) Winkler, J. R.; Netzel, T. L.; Creutz, C.; Sutin, N. Direct Observation of Metal-to-Ligand Charge-Transfer (MLCT) Excited States of Pentaammineruthenium(II) Complexes. *J. Am. Chem. Soc.* **1987**, *109*, 2381–2392.
(23) Harriman, A. Photochemistry of a Surfactant Derivative of Tris-(2,2'-bipyridyl)ruthenium(II). *J. Chem. Soc. Chem. Commun.* **1977**, 777.
(24) Juris, A.; Balzani, V.; Barigelletti, F.; Campagna, S.; Belser, P.; von Zelewsky, A. Ru(II) Polypyridine Complexes: Photophysics, Photochemistry, Eletrochemistry, and Chemiluminescence. *Coord. Chem. Rev.* **1988**, *84*, 85–277.
(25) Österman, T.; Abrahamsson, M.; Becker, H.-C.; Hammarström, L.; Persson, P. Influence of Triplet State Multidimensionality on Excited State Lifetimes of Bis-Tridentate Ru II Complexes: A Computational Study. *J. Phys. Chem. A* **2012**, *116*, 1041–1050.
(26) Kozlowska, M.; Rodziewicz, P.; Brus, D. M.; Breczko, J.; Brzezinski, K. Bis(2,2′:6′,2″-Terpyridine)Ruthenium(II) Bis(Perchlorate) Hemihydrate. *Acta Crystallogr. Sect. E Struct. Reports Online* **2012**, *68*, m1414–m1415.
(27) Wolpher, H.; Johansson, O.; Abrahamsson, M.; Kritikos, M. A Tridentate Ligand for Preparation of Bisterpyridine-like Ruthenium(II) Complexes with an Increased Excited State Lifetime. *Inorg. Chem. Commun.* **2004**, *7*, 337–340.
(28) Abrahamsson, M.; Jäger, M.; Österman, T.; Eriksson, L.; Persson, P.; Becker, H.; Johansson, O.; Hammarström, L. A 3.0 μs Room Temperature Excited State Lifetime of a Bistridentate Ru^{II} −Polypyridine Complex for Rod-like Molecular Arrays. *J. Am. Chem. Soc.* **2006**, *128*, 12616–12617.
(29) Ragazzon, G.; Verwilst, P.; Denisov, S. A.; Credi, A.; Jonusauskas, G.; McClenaghan, N. D. Ruthenium(II) Complexes Based on Tridentate Polypyridine Ligands That Feature Long-Lived Room-Temperature Luminescence. *Chem. Commun.* **2013**, *49*, 9110.

(30) Schroot, R.; Schlotthauer, T.; Schubert, U. S.; Jäger, M. Modular Assembly of Poly(Naphthalene Diimide) and Ru(II) Dyes for an Efficient Light-Induced Charge Separation in Hierarchically Controlled Polymer Architectures. *Macromolecules* **2016**, *49*, 2112–2123.

(31) Schlotthauer, T.; Suchland, B.; Görls, H.; Parada, G. A.; Hammarström, L.; Schubert, U. S.; Jäger, M. Aryl-Decorated Ru^{II} Polypyridyl-Type Photosensitizer Approaching NIR Emission with Microsecond Excited State Lifetimes. *Inorg. Chem.* **2016**, *55*, 5405–5416.

(32) Schramm, F.; Meded, V.; Fliegl, H.; Fink, K.; Fuhr, O.; Qu, Z.; Klopper, W.; Finn, S.; Keyes, T. E.; Ruben, M. Expanding the Coordination Cage: A Ruthenium(II)−Polypyridine Complex Exhibiting High Quantum Yields under Ambient Conditions. *Inorg. Chem.* **2009**, *48*, 5677–5684.

(33) Abrahamsson, M.; Becker, H. C.; Hammarström, L.; Bonnefous, C.; Chamchoumis, C.; Thummel, R. P. Six-Membered Ring Chelate Complexes of Ru(II): Structural and Photophysical Effects. *Inorg. Chem.* **2007**, *46*, 10354–10364.

(34) Lumpkin, R. S.; Kober, E. M.; Worl, L. A.; Murtaza, Z.; Meyer, T. J. Metal-to-Ligand Charge-Transfer (MLCT) Photochemistry: Experimental Evidence for the Participation of a Higher Lying MLCT State in Polypyridyl Complexes of Ruthenium(II) and Osmium(II). *J. Phys. Chem.* **1990**, *94*, 239–243.

(35) Turro, C.; Bossmann, S. H.; Jenkins, Y.; Barton, J. K.; Turro, N. J. Proton Transfer Quenching of the MLCT Excited State of $Ru(phen)_2dppz^{2+}$ in Homogeneous Solution and Bound to DNA. *J. Am. Chem. Soc.* **1995**, *117*, 9026–9032.

(36) Delaney, S.; Pascaly, M.; Bhattacharya, P. K.; Han, K.; Barton, J. K. Oxidative Damage by Ruthenium Complexes Containing the Dipyridophenazine Ligand or Its Derivatives: A Focus on Intercalation. *Inorg. Chem.* **2002**, *41*, 1966–1974.

(37) Alan E. Friedman, J.-C. C.; Jean-Pierre Sauvage, Nicholas J. Turro, And Barton·, J. K. Molecular "Light Switch" for DNA: $Ru(bpy)_2(dppz)^{2+}$. *J. Am. Chem. Soc.* **1990**, *2*, 4960–4962.

(38) McKinley, A. W.; Lincoln, P.; Tuite, E. M. Sensitivity of $[Ru(phen)_2dppz]^{2+}$ Light Switch Emission to Ionic Strength, Temperature, and DNA Sequence and Conformation. *Dalton Trans.* **2013**, *42*, 4081.

(39) Choudhuri, M. M. R.; Behzad, M.; Al-Noaimi, M.; Yap, G. P. A.; Kaim, W.; Sarkar, B.; Crutchley, R. J. Variable Noninnocence of Substituted Azobis(Phenylcyanamido)Diruthenium Complexes. *Inorg. Chem.* **2015**, *54*, 1508–1517.

(40) Hu, Y.; Wilson, M. H.; Zong, R.; Bonnefous, C.; McMillin, D. R.; Thummel, R. P. A Luminescent Pt(II) Complex with a Terpyridine-like Ligand Involving a Six-Membered Chelate Ring. *Dalt. Trans.* **2005**, No. 2, 354

(41) Bolger, J.; Gourdon, A.; Ishow, E.; Launay, J. Mononuclear and Binuclear Tetrapyrido[3,2-a :2',3'- c :3",2"- H :2'",3'"- j]phenazine (tpphz) Ruthenium and Osmium Complexes. *Inorg. Chem.* **1996**, *35*, 2937–2944.

(42) (a) Ito, A.; Meyer, T. J. The Golden Rule. Application for Fun and Profit in Electron Transfer, Energy Transfer, and Excited-State Decay. *Phys. Chem. Chem. Phys.* **2012**, *14*, 13731. (b) Allen, G. H.; White, R. P.; Rillema, D. P.; Meyer, T. J. Synthetic Control of Excited-State Properties. Tris-Chelate Complexes Containing the Ligands 2,2'-Bipyrazine, 2,2'-Bipyridine, and 2,2'-Bipyrimidine. *J. Am. Chem. Soc.* **1984**, *106*, 2613–2620. (c) Caspar, J. V.; Westmoreland, T. D.; Allen, G. H.; Bradley, P. G.; Meyer, T. J.; Woodruff, W. H. Molecular and Electronic Structure in the Metal-to-Ligand Charge Transfer Excited

States of d^6 Transition-Metal Complexes in Solution. *J. Am. Chem. Soc.* **1984**, *106*, 3492–3500.
(43) Demas, J. N.; Harris, E. W.; McBride, R. P. Energy Transfer from Luminescent Transition Metal Complexes to Oxygen. *J. Am. Chem. Soc.* **1977**, *99*, 3547–3551.
(44) Nair, R. B.; Teng, E. S.; Kirkland, S. L.; Murphy, C. J. Synthesis and DNA-Binding Properties of $[Ru(NH_3)_4dppz]^{2+}$. *Inorg. Chem.* **1998**, *37*, 139–141.
(45) Sun, Y.; Lutterman, D. A.; Turro, C. Role of Electronic Structure on DNA Light-Switch Behavior of Ru(II) Intercalators. *Inorg. Chem.* **2008**, *47*, 6427–6434.
(46) Liu, Y.; Hammitt, R.; Lutterman, D. A.; Thummel, R. P.; Turro, C. Marked Differences in Light-Switch Behavior of Ru(II) Complexes Possessing a Tridentate DNA Intercalating Ligand. *Inorg. Chem.* **2007**, *46*, 6011–6021.
(47) Sun, Q.; Mosquera-Vazquez, S.; Suffren, Y.; Hankache, J.; Amstutz, N.; Lawson Daku, L. M.; Vauthey, E.; Hauser, A. On the Role of Ligand-Field States for the Photophysical Properties of Ruthenium(II) Polypyridyl Complexes. *Coord. Chem. Rev.* **2015**, *282–283*, 87–99.
(48) Lumpkin, R. S.; Kober, E. M.; Worl, L. A.; Murtaza, Z.; Meyer, T. J. Metal-to-Ligand Charge-Transfer (MLCT) Photochemistry: Experimental Evidence for the Participation of a Higher Lying MLCT State in Polypyridyl Complexes of Ruthenium(II) and Osmium(II). *J. Phys. Chem.* **1990**, *94* (1), 239–243.
(49) Litke, S. V.; Ershov, A. Y.; Meyer, T. J. Photophysics of Bis-Bipyridyl Nitro Complexes of Ruthenium(II) with Pyridine Ligands: Substituent Effects. *J. Phys. Chem. A* **2014**, *118*, 6216–6222.
(50) Winkler, J. R.; Netzel, T. L.; Creutz, C.; Sutin, N. Direct Observation of Metal-to-Ligand Charge-Transfer (MLCT) Excited States of Pentaammineruthenium(II) Complexes. *J. Am. Chem. Soc.* **1987**, *109*, 2381–2392.
(51) Amini, A.; Harriman, A.; Mayeux, A. The Triplet Excited State of Ruthenium(II) Bis(2,2':6',2''-terpyridine): Comparison Between Experiment and Theory. *Phys. Chem. Chem. Phys.* **2004**, *6*, 1157-1164.
(52) Barigelletti, F.; Juris, A.; Balzani, V. Belser, P.; von Zelewsky, A. Temperature Dependence of the Bis(2,2'-bipyridine)dicyanoruthenium(II) and Bis(2,2'-bipyridine)(2,2'-isobiquinoline)ruthenium(II) Luminescence. *Phys. Chem. Chem. Phys.* **1987**, 1095–1098.
(53) Abrahamsson, M.; Jäger, M.; Kumar, R. J.; Österman, T.; Persson, P.; Becker, H.-C.; Johansson, O.; Hammarström, L. Bistridentate Ruthenium(II)Polypyridyl-Type Complexes with Microsecond ^{3}MLCT State Lifetimes: Sensitizers for Rod-Like Molecular Arrays. *J. Am. Chem. Soc.* **2008**, *130*, 15533–15542.
(54) Thompson, D. W.; Fleming, C. N.; Myron, B. D.; Meyer, T. J. Rigid Medium Stabilization of Metal-to-Ligand Charge Transfer Excited States. *J. Phys. Chem. B* **2007**, *111*, 6930–6941
(55) Murtaza, Z.; Graff, D. K.; Zipp, A. P.; Worl, L. A.; Jones, Jr., W. E.; Bates, W. D.; Meyer, T. J. Energy Transfer in the Inverted Region: Calculation of Relative Rate Constants by Emission Spectral Fitting. *J. Phys. Chem.* **1994**, *98*, 10504–10513.
(56) Klassen, D. M.; DelPup, R. V. Excited State Properties of Mixed Phosphine 2-(2'-Pyridyl)Quinoline Complexes of Ruthenium(II). *Inorg. Chem.* **2002**, *41*, 3155–3160.
(57) Rohrabaugh, T. N.; Collins, K. A.; Xue, C.; White, J. K.; Kodanko, J. J.; Turro, C. New Ru(II) Complex for Dual Photochemotherapy: Release of Cathepsin K Inhibitor and $^1O_2$ Production. *Dalton Trans.* **2018**, *47*, 11851–11858.

(58) Zhao, R.; Hammitt, R.; Thummel, R. P.; Liu, Y.; Turro, C.; Snapka, R. M. Nuclear Targets of Photodynamic Tridentate Ruthenium Complexes. *Dalton Trans.* **2009**, 10926.
(59) Sun, Y.; Joyce, L. E.; Dickson, N. M.; Turro, C. Efficient DNA Photocleavage by $[Ru(bpy)_2(dppn)]^{2+}$ with Visible Light. *Chem. Commun.* **2010**, *46*, 2426.
(60) Song, H.; Kaiser, J. T.; Barton, J. K. Crystal Structure of Δ-$Ru(bpy)_2dppz^{2+}$ Bound to Mismatched DNA Reveals Side-by-Side Metalloinsertion and Intercalation. *Nature Chem.* **2013**, *4*, 615–620.
(61) Mårtensson, A. K. F.; Lincoln, P. Competitive DNA Binding of $Ru(bpy)_2dppz^{2+}$ Enantiomers Studied with Isothermal Titration Calorimetry (ITC) Using a Direct and General Binding Isotherm Algorithm. *Phys. Chem. Chem. Phys.* **2018**, *20*, 7920–7930.
(62) Cardin, C. J.; Kelly, J. M.; Quinn, S. J. Chemical Science Photochemically Active DNA-Intercalating Ruthenium and Related Complexes – Insights by Combining Crystallography and Transient Spectroscopy. *Chem. Sci.* **2017**, *8*, 4705–4723.
(63) Phillips, T.; Haq, I.; Meijer, A. J. H. M.; Adams, H.; Soutar, I.; Swanson, L.; Sykes, M. J.; Thomas, J. A. DNA Binding of an Organic Dppz-Based Intercalator. *Biochemistry* **2004**, *43*, 13657–13665.
(64) Galindo-Murillo, R.; Cheatham, III, T. E. Ethidium Bromide Interactions with DNA: An Exploration of a Classic DNA-Ligand Complex with Unbiased Molecular Dynamics Simulations. *Nucleic Acids Res.* **2021**, *49*, 3735–3747.
(65) Görner, H.; Tossi, A. B.; Stradowski, C.; Schulte-Frohlinde, D. Binding of $Ru(bpy)_3^{2+}$ and $Ru(phen)_3^{2+}$ to Polynucleotides and DNA: Effect to Added Salts on the Absorption and Luminescence Properties. *J. Photochem. Photobiol.* **1988**, 67–89.
(66) Lincoln, P.; Nordén, B. DNA Binding Geometries of Ruthenium Complexes with 1,10-Phenanthroline and 2,2'-Bipyridine Ligands Studied with Linear Dichroism Spectroscopy. Borderline Cases of Intercalation. *J. Phys. Chem. B* **1998**, *102*, 9583–9594.